Received: 26 October 2021 | Revised: 29 November 2021 | Accepted: 16 December 2021

IET Renewable Power Generation

DOI: 10.1049/rpg2.12381

The Institution of Engineering and Technology WILEY

ORIGINAL RESEARCH PAPER

Process intensification for generating and decomposing formic acid, a liquid hydrogen carrier

Jonathan D. Egbert[1] | Katarzyna Grubel[1] | Daniel T. Howe[1] | Robert S. Weber[1] | Arun S. Agarwal[2] | Todd Brix[2]

[1] Pacific Northwest National Laboratory, Richland, Washington, USA

[2] OCOchem, Inc., 350 Hills Street, Richland, Washington, USA

Correspondence
Robert S. Weber, Pacific Northwest National Laboratory PO Box 999, Richland, Washington 99352, USA.
Email: robert.weber@pnnl.gov

Funding information
U.S. Department of Energy, Technology Commercialization Fund; Cooperative Research and Development Agreement with OCOchem; Office of Energy Efficiency and Renewable Energy, Fuel Cell Technology Office; Pacific Northwest National Laboratory (PNNL), Grant/Award Number: DE-AC05-76RL01830

Abstract

The authors preview two processes that facilitate the use of formic acid (HCOOH) as a liquid hydrogen carrier to store renewably-generated electrical energy and then release it to generate electrical power cleanly for backup or emergency applications. First, we show that simultaneously oxidizing an organic solute (typically a waste stream) can assist the electrochemical synthesis of formic acid by lowering the cell potential—we call that coupling "Anode Boosting". The electrolyser comprises a hybrid 3-chamber PEM stack that reduces CO_2 via a gas-diffusion cathode boosted by the oxidation of aqueous methanol. However, the extent of the boosting needs to be optimized across the whole operation of the cell. Next, results from an intensified catalytic reactor for decomposing the formic acid back into H_2 and CO_2 at elevated pressure so that the H_2 can be used in a fuel cell is presented. The reactor combines three operations: Vaporization of the formic acid, its decomposition, and separation of the product stream. Their close coupling affords energy savings and a compact design that could be mounted on a mobile skid. The authors briefly discuss the electrode catalyst that facilitates the first process and two thermally activated catalysts (Ir supported on covalent triazine framework and Pd supported on carbon) that enable the second process.

1 | INTRODUCTION

The electrochemical reduction of CO_2 can produce formic acid, HCOOH both sustainably and cost-competitively with non-sustainable processes [1–3]. Because formic acid can be dehydrogenated to form an equimolar mixture of H_2 and CO_2 [4–8], the molecule can be considered a liquid hydrogen carrier [7, 9–13] whose economics can surpass those of compressed or liquified hydrogen when the cost of distribution is included (Table 1).

Here, we have investigated, preliminarily, how to make the production of formic acid even more frugal, and how to dehydrogenate it in a way conducive to distributed processing for use in fuelling back-up or load-levelling generation of electrical power. The production involves simultaneously oxidizing a sacrificial, waste anolyte to lower the operating potential of the electrolysis cell in which the formic acid is produced—we have termed that coupling "Anode Boosting" [16]. The dehydrogenation involves development of a reactor that combines vaporization of the formic acid with its metal-catalysed dehydrogenation, followed by membrane separation of the produced H_2 and CO_2. The connection of this work to the conversion of biomass is a bit tangential: The carbon dioxide is envisioned to come from the fermentation of sugars to make ethanol.

2 | EXPERIMENTAL

Anode boosting: The steady state electrolysis was carried out using a 10 cm^2 filter press cell employing a Nafion 117 separator (Figure 1). The cathode was 1.8–2 mg/cm^2 30 wt% Sn/C nano catalyst loaded on TORAY 120C paper. The anode was a commercial 4 mg/cm^2 Pt-Ru/Carbon electrode (Fuel Cell Store, product code 1610012–3). The cell was fed with a CO_2-saturated catholyte (2 M KCl, saturated with CO_2 using a bubbler; pH = 3.70–3.80) and an acidic anolyte

TABLE 1 Components of the cost delivering renewably produced hydrogen at a scale of 0.45 ton/day over a distance of 300 km. Numerical entries are costs in US dollars per kg of H_2

Characteristic	Formic acid	160 bar or liquid "green" H_2[d]
Production cost[a]	7.7[b]	5.0
Compression, storage and distribution cost	1[c]	10.2
Delivered cost	~9	~15
Safety	ambient P, T; nonflammable	cryogenic or high pressure; explosive

[a]Both processes involve electrochemical reduction: aqueous CO_2 (formic acid) or water (H_2).
[b]Estimate by OCOchem; compare to value of 13.6 USD/kg_{H_2} from Shin et al. [1].
[c]In 2018 [14] the average trucking revenue was 0.2020 USD ton/mile × 0.62 mi/km × 1 t_{Fa}/0.0369 t_{H_2} × 300 km.
[d]Stetson, Fuel Cell Technologies Annual Merit Review [15].

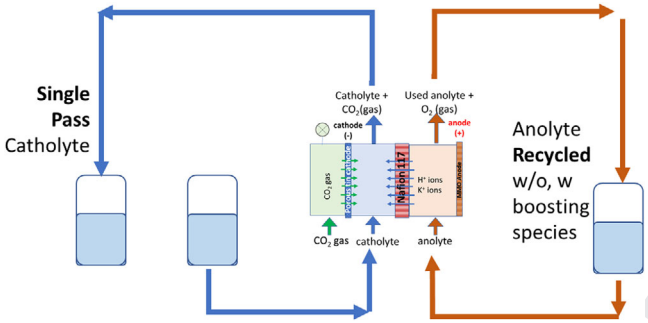

FIGURE 1 Schematic of the anolyte boosting test setup with anolyte recycle and single pass catholyte flow

TABLE 2 Anode boosting using at Pt-Ru/carbon paper anode and methanol in an anolyte containing 0.5 M H_2SO_4 and 0.5 M K_2SO_4

[Methanol] (M)	Cell current (mA/cm)	Cell potential (V)	Anode boosting (%)
0	120	4.26	—
1	120	4.29	−1
2	120	4.21	1
3	120	4.16	2
0	60	3.79	—
3	60	3.66	3.4

(H_2SO_4 + 0.5 M K_2SO_4) to which methanol was added to make 1, 2, or 3 M solutions (Table 2). The quantity of anolyte (~2 L) contained enough methanol such that the total experimental time of >60 min at the anticipated current would reduce its concentration by <1% even if 100% of the anode current is provided by oxidation of the methanol. It was observed that addition of methanol led to the precipitation of some salt, most likely K_2SO_4, which was removed by filtration.

The operating conditions were maintained constant (anolyte flowrate = 75–80 mL/min; catholyte flowrate = 10–11 mL/min; CO_2 flowrate ≈ 100 mL/min; the current densities were maintained at 60 or 120 mA/cm^2).

We further tested the dependency of anode boosting on the composition of the anolyte using an H-cell equipped with the same Pt–Ru/carbon paper anode and a tin foil cathode (each about 1 cm^2). The catholyte was CO_2-saturated 1 M $NaHCO_3$. The anolyte started as 1 M Na_2SO_4 and was diluted by addition of methanol (to make a 1 M solution). Then, sodium bicarbonate was added until the pH of the anolyte rose from 7 to 9. The potential of the cathode was swept around −1 V vs the Ag/AgCl counter electrode located adjacent to the tin electrode in the cathode half-cell. The anode voltage was measured independently vs a second Ag/AgCl electrode located adjacent to the anode in the anode half-cell. The cell current during the sweep was approximately 1 mA.

2.1 | Dehydrogenation of formic acid

In a series of preliminary experiments to demonstrate that the decomposition of formic acid could produce high pressures of H_2 and CO_2, formic acid (either 80 or 99 wt%) was charged into 59 mL Parr autoclave where it contacted either (i) a heterogeneous catalyst based on a porous organic material, Ir@covalent triazine framework [17], or (ii) a more traditional heterogenous catalyst (10 wt% Pd/carbon felt prepared by incipient wetness impregnation as described previously) [18]. The meso-porous covalent triazine framework was synthesized as described by Bavykina et al., except that we employed a small stainless steel, Swagelok "bomb" instead of a quartz ampoule for the polymerization reaction. The pressure and temperature in the batch reactor were monitored continuously; the composition of the gas phase was assayed at the end of the reaction by micro gas chromatography (micro GC).

To test continuous, high-pressure operation, a reactor consisting of a heated feed line, a catalyst section, a water-cooled condenser, and a condensate collection leg was fabricated from ½-inch, 316 stainless steel tubing and Swagelok connectors (Figure 2). The catalyst bed was packed with 1.5 g (~3 cm) of a commercial Pd/C catalyst (5 wt% Pd/C, Aldrich). The reactor was fed with 85 wt% formic acid using an HPLC pump. The flow rate of the gaseous effluent was monitored by a bubble flow meter. A slipstream, cooled to −40 °C and then passed through a column of sodium bicarbonate and dried silica gel, was analysed continuously by microGC for H_2, CO_2 and CO.

2.2 | H_2 separation

Given that the dehydrogenation reaction produces the H_2 and CO_2 at elevated pressure, we first thought to try to enrich the product stream in H_2 through the use of a nanoporous membrane that exploited the difference in rates of Knudsen diffusion of the two gases [19]. We used a 20 nm, nanoporous, titania-coated metal filter from Graver Technologies [20]. The system also included a heated water bubbler fabricated from Swagelok fittings and stainless-steel tubing that can humidify the inlet stream (Figure 3).

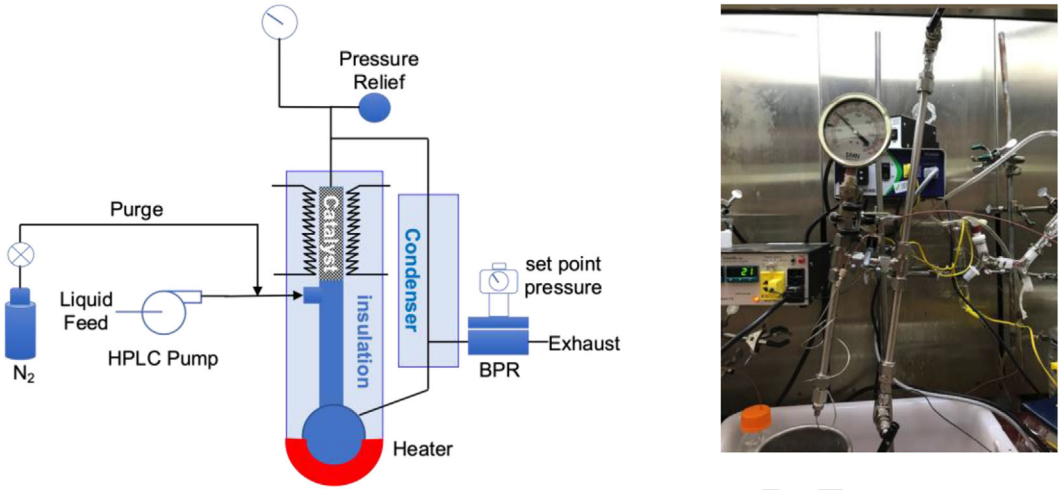

FIGURE 2 Dehydrogenation reactor. Left: Notional schematic; Right: photograph of the bench scale apparatus constructed of ½ in. stainless steel. In this prototype the products are cooled (upper right arm) and the collected condensate is blown down (through the valve on the condensate collector, lower right leg), not returned to the boiler. The temperature of the reactor (125–160 °C) was controlled using a "bath" of aluminium pellets heated with a hot plate (not shown) to conduct heat to the formic acid inlet (small bore tubing, which acted as a flash vaporizer) and the reactor chamber (lower left leg). The reactor was equipped with an overpressure rupture disk rated at 2000 psig (~140 bar)

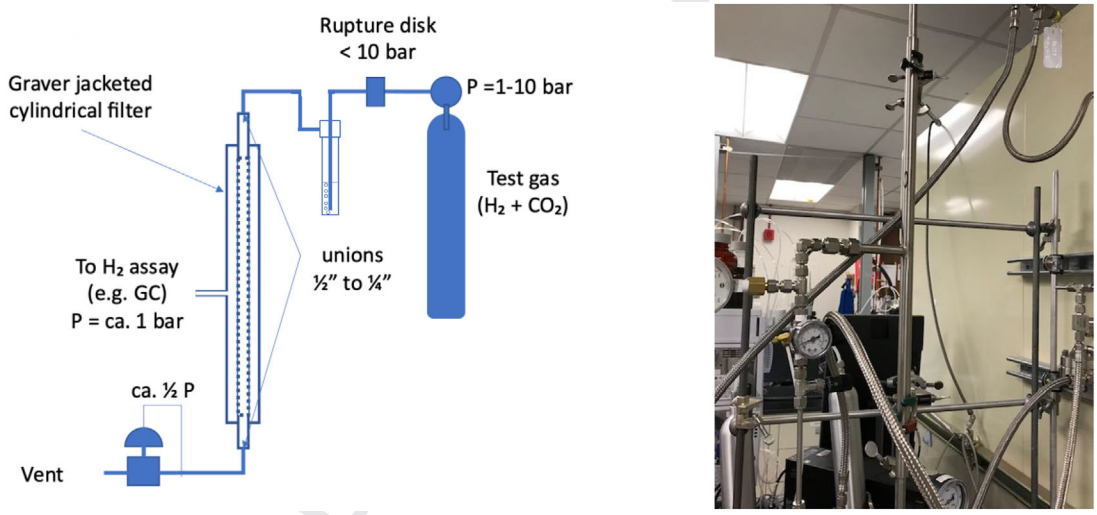

FIGURE 3 Nanoporous membrane employed to test differential Knudsen diffusion for extracting H_2 from an equimolar mixture of H_2 and CO_2. Left: system schematic; Right photograph of the apparatus. The main tube is approximately 60 cm in length

3 | RESULTS AND DISCUSSION

3.1 | Anode-boosted electrolysis of CO_2

The extent of anode boosting in the acidic electrolyte that had been optimized for the reduction of CO_2 was much smaller than we had hoped, instead of the approximately 0.5 V that would have arisen had all the free energy of methanol oxidation been available, it was just a few percent of the cell voltage. In agreement with our previous results [16], the anode boosting increased with increasing concentration of methanol and decreased with increasing cell current (Table 2).

We have previously ascribed the current dependence of anode boosting to the exclusion of the methanol from the double layer near the anode at high potentials [16]. We therefore were concerned that the sulphate anion, which is known to be kosmotropic [21, 22] (solvent ordering), may have played a role in further preventing methanol from approaching the anode. Therefore, we performed a series of quick experiments using an H-cell, in which the anolyte was successively changed to include the sacrificial anolyte (methanol) and then made basic in the presence of bicarbonate that should be less solvent ordering (Tables 3–5). Q3

While these experiments unfortunately confound the effect of the charge compensating anion (SO_4^{2-}, HCO_3^-) with the pH

TABLE 3 Further effect of the composition of the anolyte on anode boosting

Anolyte	Cell potential (V)	Anode boosting (%)
1 M Na_2SO_4	1.42	—
Above plus CH_3OH to 1 M	1.04	37
Above plus $NaHCO_3$ to pH 9	0.84	69

TABLE 4 Average final compositions (mol%, three replicates) of dried gas produced by catalytic dehydrogenation of 99 wt% formic acid

Experiment	H_2	CO_2	CO	N_2	O_2
Initial charge	48.2	50.1	0.4	1.3	0.1
First reload	48.9	49.5	0.4	1.1	0.0
Second reload	48.3	50.7	0.3	0.7	0.0

TABLE 5 Separation of H_2 and CO_2 using a nanoporous filter

Feed	S_f[a)]
Dry $H_2 + CO_2$	1.0
Slightly humidified $H_2 + CO_2$	1.04

[a)] $S_f = (CO_{2,out}/H_{2,out})/(CO_{2,in}/H_{2,in})$.

of the solution, they are consistent with the hypothesis that the double layer needs to permit the approach of the methanol (or methoxide anion) for there to be a large effect of anode boosting (Figure 4).

3.2 | Dehydrogenation of formic acid (batch experiments)

The decarboxylation of formic acid produces elevated pressures of a nearly equimolar mixture of H_2 and CO_2, with low but not negligible contamination by CO [23], when catalysed by a platinum group metal [24].

$$HCOOH \rightarrow H_2 + CO_2H_2 + CO_2$$

$$\Delta G_{reaction}\,(373K)\,[10] = -49.4$$

$$K\,(373\,K) = 8.2\,Mbar$$

We have confirmed the production of gases at high pressure (Figure 5) for both high concentrations (99 wt%) and more dilute feedstocks (80 wt%) of formic acid.

At the end of the reactions, the composition of the gas phase was H_2: 48.2 mol%, CO_2: 50.2 mol%, CO: 0.3–0.4 mol%, and balance N_2 and O_2 from residual air introduced during filling of the autoclave. The maximum pressures were limited by the charge of formic acid, chosen to stay within the safe operating pressure of the autoclave ($P < 172$ bar). The charge of concentrated formic acid (3.95 g) contained 0.085 mol of HCOOH; the charge of the more dilute formic acid (13 mL) contained 0.17 mol of HCOOH and the maximum pressure in the second experiment (158 bar) was, correspondingly, about twice as high as in the first experiment (83 bar). The difference arises from the compressibility of the vapour (both water and formic acid form dimers at higher pressure).

We tested the reuse of the supported Ir catalysts (Figure 6), which upon reloading formic acid shows a change in the kinetic profile. In all instances there was evidence for the reverse water gas shift reaction, $H_2 + CO_2 \rightarrow H_2O + CO$, possibly arising from residual acidity of the support (Table 2).

We have also tested catalysts inspired by the work of Tedsree et al., [25], which contained Pd@Ag supported on carbon felt, but found that their immersion in formic acid leached the metal.

3.3 | Dehydrogenation of formic acid (continuous experiments)

As a prelude to designing and constructing the apparatus made from metal that could operate at higher pressures, $P > 10$ bar, we fabricated a reactive distillation unit from standard glass components (Figure 7) and operated it at atmospheric pressure. For the continuous experiments we employed a commercial, Pd/C catalyst with the hope that it would prove as active and durable as the Ir-based catalyst but with a less expensive metal.

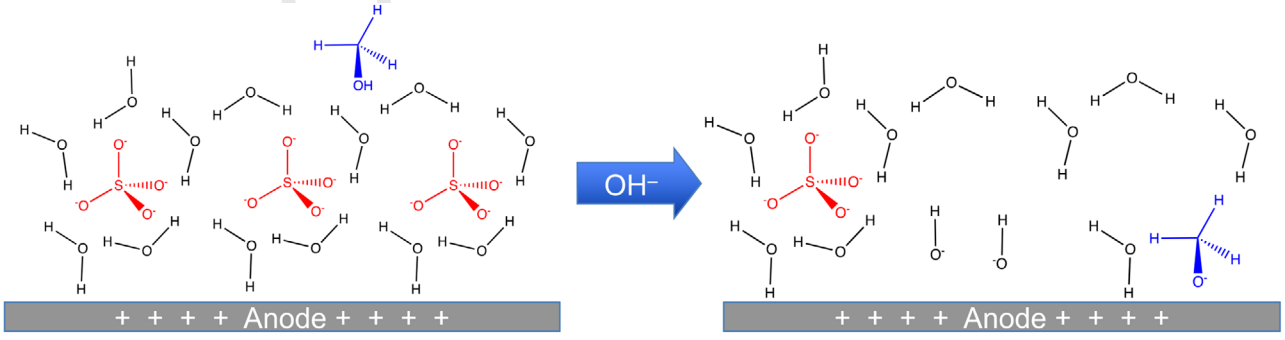

FIGURE 4 Anode boosting requires the sacrificial anolyte to be able to approach the anode, which is impeded by a kosmotropic anion like sulphate and enhanced by a chaotropic anion like hydroxide

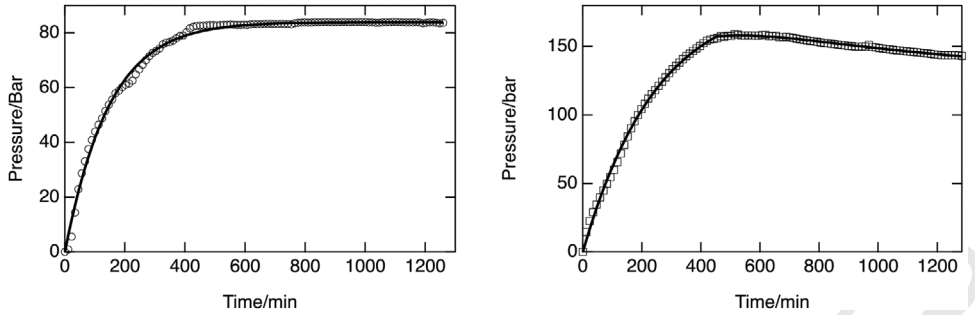

FIGURE 5 Left: Dehydrogenation of 99% formic acid catalyzed by unsupported Ir@covalent triazine framework performed in an autoclave at 120 °C; Right: Dehydrogenation of 80 wt% formic acid catalysed by the Ir complex supported on carbon felt under the same conditions. Open symbols are the measured pressures at the indicated times. The solid curves are a 1st order kinetic fits to the data that accounts for the non-ideality of the vapour at the reaction temperature

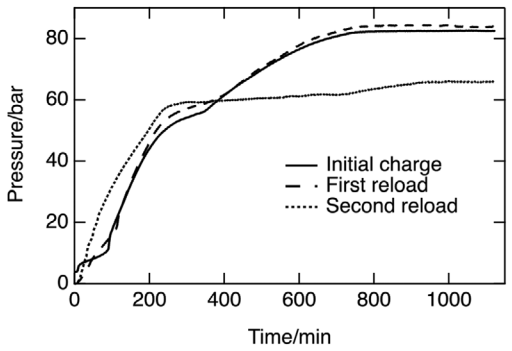

FIGURE 6 Re-use of the felt-supported Ir catalyst. Initial and subsequent charges were 3.95 mL of 99 wt% formic acid

FIGURE 7 Photograph of the glass version of the reactive distillation unit. The catalyst was positioned in the heat traced column. The condensate was periodically sampled as was the gas composition

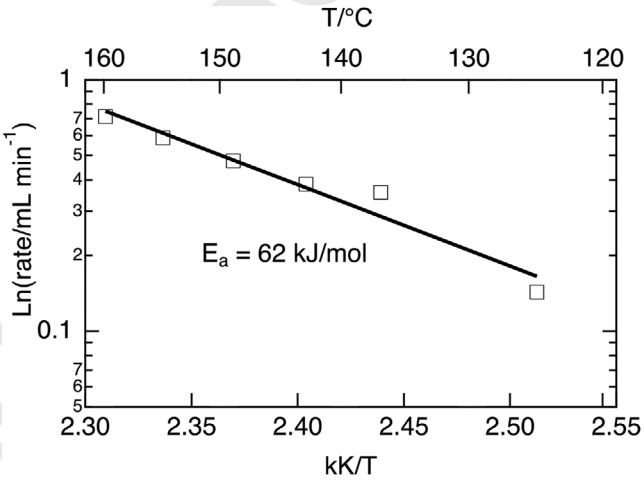

FIGURE 8 Apparent activation energy for the dehydrogenation of formic acid over a 5 wt% Pd/C catalyst

With the glass system we could easily change the catalysts, independently control the rate of evaporation of the aqueous formic acid, and the temperature of the catalyst.

With both the pot temperature and the catalyst temperature set at 130 °C, the system produced 5.7 mL/s of gas whose composition was ~50 mol% H_2, ~50 mol% CO_2 and 0.7 mol% CO when we used the commercial Pd/C catalyst (5 wt% Pd/C, Aldrich; estimated fractional exposure of the Pd = 25%). That rate of production corresponds to a turnover frequency (mol H_2/mol Pd) of ~1 Hz, which is comparable to the values found in the [26] (0.24–0.35 Hz) when all the data are extrapolated to 130 °C using an apparent activation energy of 66 kJ/mol. It is also verging on a reaction rate that could be limited by finite rates of transport of the reactants, or products, to/from the catalyst. The amount of CO decreased when the catalyst operated at higher temperatures (>140 °C). When operated at low pressures and at low flow rates of the 85 wt% formic acid feed, 0.015 mL/min, the catalyst and reactor produced the nearly equimolar mixture of H_2 and CO_2, for over 18 h.

The commercial 5 wt% Pd/C catalyst, when operated at a feed rate of 0.24 mL/min, temperatures between 125–160 °C, and atmospheric pressures produced a nearly equimolar mixture of H_2 and CO_2 (CO varied from 2 to 0.5 mol%), with an apparent activation energy for the dehydrogenation reaction of 62 kJ/mol (Figure 8).

We note that there is precedent for a compact dehydrogenation unit [6, 7, 9]. Here we are specifically targeting a unit that capable of operating at elevated pressure to feed a membrane separator and, ultimately, to refuel a hydrogen-fuelled vehicle.

H2 separation: As expected [19], the nanoporous filter did not separate a dry stream of H_2 and CO_2. It exhibited only a slight separation, Sf = $(CO_{2,out}/H_{2,out})/(CO_{2,in}/H_{2,in})$, when fed with gases that had bubbled through water at room temperature (Table 3). We infer that water adsorbed on the metal oxide coating and dissolved the CO_2, which then diffused across the membrane to be equilibrated with the gas at lower pressure. To further purify the hydrogen, we will operate the current membrane at a higher level of humidification, and we are preparing to test a commercial, polymeric membrane separator.

4 | CONCLUSIONS

Dehydrogenation of formic acid can produce high pressure hydrogen for use in a downstream fuel cell. However, both the generation of the formic acid and its decomposition require attention to improve the energetics and selectivity of the processes. The former may include the use of anode boosting; the latter requires both a more selective catalyst and a more effective separations protocol than those detailed here, especially if the production of CO proves unavoidable. Both processes include elements of process intensification. We hesitate to infer much more from these preliminary experiments, which were designed only to explore operation at high pressures, not typically reported in the literature.

CONFLICT OF INTEREST

None.

DATA AVAILABILITY STATEMENT

The data that support the findings of this study are available from the corresponding author upon reasonable request.

FUNDING SOURCES

The work on the dehydrogenation reactor and hydrogen purification was supported by the U.S. Department of Energy, Technology Commercialization Fund through a Cooperative Research and Development Agreement with OCOchem; the work on anode boosting was supported by Office of Energy Efficiency and Renewable Energy, Fuel Cell Technology Office with cost-sharing by OCOchem, Inc. Pacific Northwest National Laboratory (PNNL) is a multiprogram national laboratory operated for DOE by Battelle under Contract DE-AC05-76RL01830.

ORCID

Jonathan D. Egbert https://orcid.org/0000-0003-3731-8461

REFERENCES

1. Shin, H., Hansen, K., U, F.J.: Techno-economic analysis of low-temperature CO_2 electrolysis processes. Nat. Sustainability 4, 911–919 (2021) https://doi.org/10.1038/s41893-021-00739-x
2. Jouny, M., Luc, W., Jiao, F.: General techno-economic analysis of CO_2 electrolysis systems. Ind. Eng. Chem. Res. 57, 2165–2177 (2018) https://doi.org/10.1021/acs.iecr.7b03514
3. Weber, R.S.: Effective use of renewable electricity for making renewable fuels and chemicals. ACS Catal. 9(2), 946–950 (2019) https://doi.org/10.1021/acscatal.8b04143
4. Tingey, H.C., Hinshelwood, C.N.: The catalytic decomposition of formic acid on surfaces of platinum and silver. J. Chem. Soc. Trans. 121, 1668–1676 (1922) https://doi.org/10.1039/CT9222101668
5. Iglesia, E., Boudart, M.: Decomposition of formic acid on copper, nickel and copper-nickel alloys I. preparation and characterization of catalysts. J. Catal. 81, 204–213 (1983)
6. Fellay, C., Dyson, P.J., Laurenczy, G.: A viable hydrogen-storage system based on selective formic acid decomposition with a ruthenium catalyst. Angew. Chem. Int. Ed. Engl. 47, 3966–3968 (2008) https://doi.org/10.1002/anie.200800320
7. Laurenczy, G., Fellay, C., Dyson, P.: Hydrogen production from formic acid. (2008) Q5
8. Ojeda, M., Iglesia, E.: Formic acid dehydrogenation on Au-based catalysts at near-ambient temperatures. Angew. Chem. Int. Ed. Engl. 48, 4800–4803 (2009) https://doi.org/10.1002/anie.200805723
9. Grasemann, M., Laurenczy, G.: Formic acid as a hydrogen source – recent developments and future trends. Energy Environ. Sci. 5, 8171–8181 (2012) https://doi.org/10.1039/c2ee21928j
10. Eppinger, J., Huang, K.-W.: Formic acid as a hydrogen energy carrier. ACS Energy Lett. 2(1), 188–195 (2016) https://doi.org/10.1021/acsenergylett.6b00574
11. Müller, K., Brooks, K., Autrey, T.: Hydrogen storage in formic acid: A comparison of process options. EnergyFuels 31, 12603–12611 (2017) https://doi.org/10.1021/acs.energyfuels.7b02997
12. Guo, J., Yin, C.K., Zhong, D.L., Wang, Y.L., Qi, T. Liu, G.H., Shen, L.T., Zhou, Q.S., Peng, Z.H., Yao, H., Li, X.B.: Formic acid as a potential on-board hydrogen storage method: Development of homogeneous noble metal catalysts for dehydrogenation reactions. ChemSusChem 14, 2655–2681 (2021) https://doi.org/10.1002/cssc.202100602
13. Kar, S., Rauch, M., Leitus, G., Ben-David, Y., Milstein, D.: Highly efficient additive-free dehydrogenation of neat formic acid. Nat. Catal. 4, 193–201 (2021) https://doi.org/10.1038/s41929-021-00575-4
14. U.S. Bureau of Transportation Statistics: Average freight revenue per ton-mile. (2020). Accessed 4 August 2021 Q6
15. Stetson, N.: Hydrogen technologies overview. (2021). Accessed 18 October 2021
16. Andrews, E.M., Egbert, J.D., Sanyal, U., Holladay, J.D., Weber, R.S.: Anode-boosted electrolysis in electrochemical upgrading of bio-oils and in the production of H_2. Energy Fuels 34, 1162–1165 (2020) https://doi.org/10.1021/acs.energyfuels.9b02524
17. Bavykina, A.V., Goesten, M.G., Kapteijn, F., Makkee, M., Gascon, J.: Efficient production of hydrogen from formic acid using a covalent triazine framework supported molecular catalyst. ChemSusChem 8, 809–812 (2015) https://doi.org/10.1002/cssc.201403173
18. Egbert, J.D., Thomsen, E.C., O'Neill-Slawecki, S.A., Mans, D.M., Leitch, D.C., Edwards, L.J., Wade, C.E., Weber, R.S.: Development and scale-up of continuous electrocatalytic hydrogenation of functionalized nitro arenes, nitriles, and unsaturated aldehydes. Org. Process Res. Dev. 23, 1803–1812 (2019) https://doi.org/10.1021/acs.oprd.8b00379
19. Shimonosono, T., Imada, H., Maeda, H., Hirata, Y.: Separation of hydrogen from carbon dioxide through porous ceramics. Materials 9(11), 930 (2016)
20. Graver Technologies. Scepter® tubular MF and UF modules, (2021). Accessed 19 October 2021
21. Marcus, Y.: Preferential solvation in mixed solvents, Part 8. Aqueous methanol from sub-ambient to elevated temperatures. Phys. Chem. Chem. Phys. 1, 2975–2983 (1999)
22. Marcus, Y.: Effect of ions on the structure of water: structure making and breaking. Chem. Rev. 109, 1346–1370 (2009)
23. Yasaka, Y., Yoshida, K., Wakai, C., Matubayasi, N., Nakahara, M.: Kinetic and Equilibrium Study on Formic Acid Decomposition in Relation to the Water-Gas-Shift Reaction. J. Phys. Chem. A 110, 11082–11090 (2006)
24. Solymosi, F., Koós, Á., Liliom, N., Ugrai, I.: Production of CO-free H_2 from formic acid. A comparative study of the catalytic behavior of Pt metals on a carbon support. J. Catal. 279(1), 213–219 (2011) https://doi.org/10.1016/j.jcat.2011.01.023

25. Tedsree, K., Li, T., Jones, S., Chan, C.W., Yu, K.M., Bagot, P.A., Marquis, E.A., Smith, G.D., Tsang, S.C.: Hydrogen production from formic acid decomposition at room temperature using a Ag-Pd core-shell nanocatalyst. Nat. Nanotechnol. 6, 302–307 (2011) https://doi.org/10.1038/nnano.2011.42
26. Bulushev, D.A., Beloshapkin, S., Ross, J.R.H.: Hydrogen from formic acid decomposition over Pd and Au catalysts. Catal. Today 154, 7–12 (2010) https://doi.org/10.1016/j.cattod.2010.03.050

How to cite this article: Egbert, JD., Grube, K., Howe, D.T., Weber, R.S., Agarwal, A.S., Brix, T.: Process Intensification for generating and decomposing formic acid, a liquid hydrogen carrier. IET Renew. Power Gener. 1–7 (2021). https://doi.org/10.1049/rpg2.12381.